ELSEVIER

Signal Processing 38 (1994) 143–151

SIGNAL PROCESSING

Morphological reduction of skeleton redundancy

Renato Kresch*, David Malah

Department of Electrical Engineering, Technion-Israel Institute of Technology, Haifa 32000, Israel

Received 3 September 1993; revised 1 December 1993

Abstract

In this work we study *morphological* methods to reduce the amount of redundant points in the Skeleton representation of images. The advantage of removing redundant points using *morphological operations only* lies in the computational efficiency of these operations, when implemented on parallel machines. We propose a classification of redundant points of the skeleton into several categories and apply this classification in the framework of a generic approach which we present for obtaining redundancy-reduced Skeletons. This approach is shown to yield morphological closed formulae for reduced Skeletons which have less redundant points than the ordinary Skeleton. The approach is also extended for reducing the redundancy in Multi-Structuring-Element Skeletons (MSES). Although complete removal of the redundancy has not been achieved yet for the general case, the generic approach is shown to provide a complete removal of skeleton points belonging to most of the redundancy categories, as well as a redundancy-free representation for a particular important case of the MSES.

Zusammenfassung

In dieser Arbeit untersuchen wir *morphologische* Methoden, um die Anzahl von redundanten Punkten in Skelettrepräsentation von Bildern zu reduzieren. Der Vorteil des Entfernens von redundanten Punkten nur durch morphologische Operationen liegt in der Effizienz der Berechnung dieser Operationen wenn sie auf parallelen Maschinen implementiert werden. Wir schlagen eine Klassifikation von redundanten Punkten des Skeletts in verschiedene Kategorien vor und wenden diese Klassifikation im Rahmen eines generischen Ansatzes, den wir vorstellen, um redundanz-reduzierte Skelette zu erhalten. Dieser Ansatz bringt morphologische Schließungsformeln für reduzierte Skelette hervor, die weniger redundante Punkte als gewöhnliche Skelette haben. Dieser Ansatz wird auch erweitert, um die Redundanz von Skeletten aus mehrfache Strukturelementen (MSES) zu reduzieren. Obwohl die vollständige Entfernung der Redundanz für den allgemeinen Fall noch nicht erreicht werden konnte, liefert der generische Ansatz eine vollständige Entfernung von Skelettpunkten, die zu den am meisten redundanten Kategorien gehören und ebenfalls eine redundanzfreie Repräsentation für einen besonders wichtige Fall eines MSES.

Résumé

Ce travail étudie des méthodes morphologiques pour réduire la redondance des points du squelette. L'avantage d'utiliser uniquement des opérations morphologiques pour éliminer les points redondants réside dans le faible coût de calcul résultant, si ces opérations sont implémentées sur des machines parallèles. On propose une classification des points redondants du squelette en plusieurs catégories et on utilise cette classification dans le cadre du calcul de squelettes

*Corresponding author.

0165-1684/94/$7.00 © 1994 Elsevier Science B.V. All rights reserved
SSDI 0165-1684(94)00024-T

à redondance réduite. Cette approche fournit des formules morphologique permettant d'obtenir des squelettes possédant moins de points redondant que les squelettes ordinaires. L'approche est également étendue à la réduction de redondance de squelettes à éléments structurants multiples (MSES). Bien que l'élimination complète de la redondance n'a pas pu être obtenue dans le cas général, on montre que l'approche permet l'élimination complète des points appartenant à la plus part des classes de redondance ainsi que obtention d'une représentation sans redondance d'un cas important de MSES.

Key words: Mathematical morphology; Skeleton; Parallel implementation; Redundancy reduction; Shape representation; Image coding; Shape analysis

1. Introduction

The morphological skeleton is a *compact* error-free representation of images, a property useful for image analysis and lossless image data compression [4,10].

However, some authors have noted the fact that the skeleton is a *redundant representation*, i.e., some of its points may be discarded without affecting its error-free characteristic. In some applications, such as coding, no importance is attributed to the skeleton *shape* or its *connectivity*, but only to its *ability to fully represent images in a compact way*. In such applications, it is of interest to remove redundant skeleton points, so that the representation contains as few as possible points.

For this purpose, Maragos and Schafer defined in [4] a *Minimal Skeleton* as being any set of points from the skeleton which *fully represents* the original image and does not so if any of its points is removed. A minimal skeleton always exists, since in the worst case it is the skeleton itself, but usually it is not unique, i.e., there can be more than one minimal skeleton for a given image.

Maragos and Schafer propose in [4] an algorithm for finding a minimal skeleton from the skeleton representation of a binary image. However, this algorithm is not fully morphological and therefore cannot be efficiently implemented on a parallel machine, in contrast to the morphological skeleton itself which is amenable to a parallel implementation. A fully morphological algorithm for finding minimal skeletons could take advantage of the parallel properties of the morphological operations and perform the computation in a more efficient way.

Another important related topic is the 'Reduced Skeleton' defined by Maragos in [3] (see also [1]). The reduced skeleton has fewer representation points than the ordinary skeleton and it is also error-free. It is not a minimal skeleton but it is obtained by morphological operations only. (The mathematical definition is reviewed in Section 2). Other efficient morphological representations are studied in [5–9].

The paper is organized as follows: in Section 2 we propose a classification of redundant points into several categories and apply this classification in the framework of a generic approach which we present for obtaining 'general' morphological error-free reduced skeletons. In particular, we show how to use this approach to obtain reduced skeletons with no redundant points in most of those redundancy categories. This method gives not only Maragos' reduced skeleton, as a particular case, but also leads to a reduced skeleton which has less skeleton points and is still error-free. In Section 3, the generic approach is extended for reducing *Multi-Structuring-Element Skeletons* (MSES) as well. We first present the definition of MSES (which was recently introduced in [2]), indicate how to obtain a *reduced* MSES, and present a particular case of the MSES for which the approach leads to a redundancy-free representation (minimal MSES).

2. Reduced skeletons

The concepts discussed in this paper are suitable for both binary and grayscale images. However, to simplify the presentation we consider here only the

binary case. The images may be continuous sets (sets in $\mathbb{R}^2$) or discrete sets (sets in $\mathbb{Z}^2$).

2.1. Types of redundant points

Let us consider a collection of subsets $\{T_n\}$ which represents a given binary image X in the following way:

$$X = \bigcup_n T_n \oplus A(n), \tag{1}$$

where $\oplus$ stands for morphological dilation, and $\{A(n)\}$ is a given family of shapes, satisfying the following increasing property: $n > m \Rightarrow A(n) \supseteq A(m)$. The parameter n may assume all the non-negative continuous values (if X and B are continuous sets) or it may assume only discrete values $n = 0, 1, \ldots$ (for X and B which are both continuous or both discrete).

A point t belonging to the subset of order n, $t \in T_n$, represents an element $A(n)$ translated to t:

$$\{t\} \oplus A(n) = A(n)_t, \tag{2}$$

where $A(n)_t \triangleq \{t + a \mid a \in A(n)\}$.

If $t \in T_n$ is *redundant*, then the element it represents ($A(n)_t$) is contained in a region represented by some or all the other representation points, i.e.,

$$A(n)_t \subseteq \left(\bigcup_{m \neq n} T_m \oplus A(m) \right) \cup [(T_n - \{t\}) \oplus A(n)]. \tag{3}$$

We propose to classify each of the redundant points into one or more of the following *redundancy categories*:

Single-element redundancy

If there exists at least *one* element *bigger* than $A(n)$ that covers $A(n)_t$, i.e.,

$$\exists m > n, \quad \exists z \mid A(n)_t \subseteq A(m)_z. \tag{4}$$

Future-level redundancy

If there exists a *union* of elements *bigger* than $A(n)$ that covers $A(n)_t$, i.e.,

$$A(n)_t \subseteq \bigcup_{m > n} T_m \oplus A(m). \tag{5}$$

Note that every 'single-element' redundant point is also a 'future-level' redundant point.

Past-level redundancy

If there exists a *union* of elements *smaller* than $A(n)$ that covers $A(n)_t$, i.e.,

$$A(n)_t \subseteq \bigcup_{m < n} T_m \oplus A(m). \tag{6}$$

Interlevel redundancy

If there exists a union of elements with size *different* from n that covers $A(n)_t$, i.e.,

$$A(n)_t \subseteq \bigcup_{m \neq n} T_m \oplus A(m). \tag{7}$$

Hence, every future-level or past-level redundant point is also an interlevel redundant point.

Intralevel redundancy

If the redundant point is not interlevel redundant, i.e.,

$$A(n)_t \not\subseteq \bigcup_{m \neq n} T_m \oplus A(m). \tag{8}$$

In this case, *every* set of elements (excluding $A(n)_t$) that covers $A(n)_t$ contains at least one element of size n.

2.2. The morphological skeleton and its redundancy

The Generalized morphological skeleton representation of a binary image X (see [1]) is the collection of sets $\{S_n\}$ given by

$$S_n = X \ominus A(n) - [X \ominus A(n)] \circ B(n), \tag{9}$$

where $\{B(n)\}$ is any given series of shapes, and the family of elements $\{A(n)\}$ is generated from $\{B(n)\}$ by the relation

$$A(0) = \{(0,0)\},$$

$$A(n + \Delta n) = A(n) \oplus B(n), \quad n \geq 0. \tag{10}$$

In (10), $\Delta n = dn$ (an infinitesimally small number) if n is continuous, or $\Delta n = 1$ if n assumes only natural

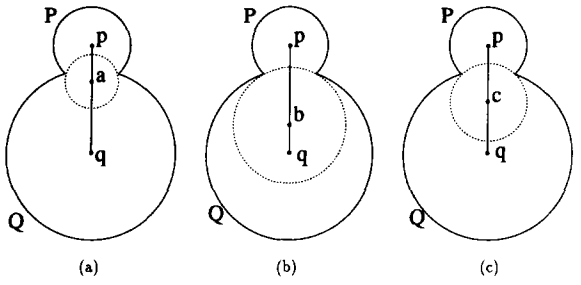

Fig. 1. Types of redundant points in the skeleton. (a) A binary image composed by two disks (P and Q), and its skeleton (the segment $[p,q]$). The point a is a 'future level' redundant point, (b) the point b is an 'interlevel' redundant point, and (c) the point c is an 'intralevel' redundant point.

values. The symbols $\ominus$ and $\circ$ denote binary erosion and opening, respectively. The minus sign in (9) denotes here *set-difference.*

The sets $\{S_n\}$ are called *skeleton subsets of order* n, and satisfy (1) for $T_n = S_n$, $\forall n$.

It is well known that the skeleton, being the set of points which are centers of maximal elements, does not contain redundant points from the 'single-element' category, i.e., it does not contain 'single-element redundancy'. On the other hand, it may contain redundant points from all the other categories.

For demonstration, Fig. 1 shows a continuous binary image composed by the union of two disks, P and Q, which are centered at the points p and q, respectively. The skeleton of the shape, computed with $B(n) = B$ (constant) equal to an infinitesimally small disk, and for continuous values of n, is the segment $[p,q]$. In this case, all the skeleton points are redundant, except for p and q. The point a in Fig. 1(a) is a 'future-level' redundant point, because the element it represents (the dotted disk) is contained in the union of two bigger maximal disks (P and Q). The point b in Fig. 1(b) is 'interlevel' redundant, because it represents a disk (the dotted one) which in this example is contained in the union of a bigger maximal disk (Q) and a smaller maximal disk (P). The point c in Fig. 1(c) is 'intralevel' redundant, because the dotted disk, which it represents, is contained in the union of a larger maximal disk (Q) and a maximal disk with the same size (P), and it is not contained in any union of only larger and smaller maximal disks.

2.3. The proposed generic approach to obtain reduced skeletons

In [4,8], the approach used to remove redundant points from the skeleton was *first* to calculate the skeleton and *then* to apply a reduction algorithm to remove the redundant points.

However, we note that the skeletonization itself is a *partial reduction process*, as we demonstrate below. If the skeleton subsets S_n would have been defined as $S_n = X \ominus A(n)$, $\forall n$, then the exact reconstruction property (1), for $T_n = S_n$, would still be satisfied, but this 'skeleton' would contain too many points. In fact, S_0 itself would then be equal to X. Instead, the sets $[X \ominus A(n)] \circ B(n)$ of redundant points are removed from $X \ominus A(n)$ for all n in the definition of the skeleton (9), so that a compact representation is obtained. However, as mentioned before, only the 'single-element redundancy' is removed this way.

We propose to remove as many redundant points as possible *during* the skeletonization process, which is fully morphological, so that a more efficient error-free decomposition than the ordinary skeleton is obtained by morphological operations only.

The proposed approach is based on the following relation:

$$RS_n = \begin{pmatrix} \text{representation} \\ \text{points of order} \\ n \end{pmatrix} - \begin{pmatrix} \text{redundant} \\ \text{points of} \\ \text{order } n \end{pmatrix}, \tag{11}$$

where $\{RS_n\}$ are the *reduced skeleton subsets.*

When the representation points are the centers of elements $A(n)$, the above relation can be written as follows:

$$RS_n = \begin{pmatrix} \text{representation} \\ \text{region of order} \\ n \end{pmatrix} \ominus A(n) - \begin{pmatrix} \text{redundant} \\ \text{region of} \\ \text{order } n \end{pmatrix} \ominus A(n). \tag{12}$$

Usually, the 'representation region of order n' is $X \circ A(n)$. By replacing the field 'redundant region

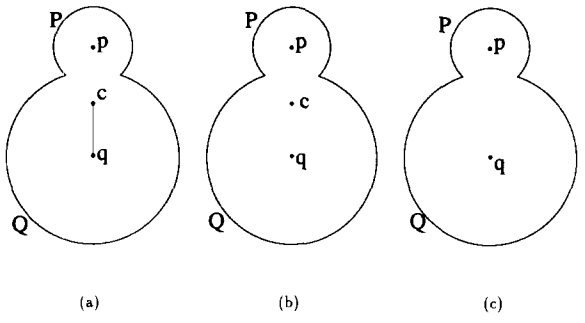

Fig. 2. (a) The same binary image as shown in Fig. 1, and its reduced skeleton $RS^{(1)}$, (b) its reduced skeleton $RS^{(2)}$, (c) its unique minimal skeleton.

of order n' in (12) by appropriate sets, one can obtain different reduced skeletons.

A skeleton with *no 'future-level redundancy'* is obtained if we choose 'redundant region' to be the *union* of all the *maximal elements* with size *greater* than n, which we denote F_n. A simple formula for obtaining F_n *before* the calculation of the elements with size greater than n is provided by the partial reconstruction relation satisfied by the skeleton subsets (see [1, 4]):

$$\bigcup_{m=k}^{\infty} S_m \oplus A(m) = X \circ A(k). \tag{13}$$

By setting $k = n + \Delta n$ in (13), we obtain

$$F_n \triangleq \bigcup_{m>n} S_m \oplus A(m) = X \circ A(n + \Delta n). \tag{14}$$

The subsets $RS_n^{(1)}$ of the resulting reduced skeleton with no 'future-level' redundancy are therefore given by

$$RS_n^{(1)} \triangleq [X \circ A(n)] \ominus A(n) - [X \circ A(n + \Delta n)] \ominus A(n). \tag{15}$$

After some simple manipulations on (15), we obtain

$$RS_n^{(1)} = X \ominus A(n) - [(X \ominus A(n)) \circ B(n)] \bullet A(n), \tag{16}$$

which is the reduced skeleton proposed by Maragos in [3] (the symbol $\bullet$ denotes binary closing). In [3], $B(n)$ is constant and equal to B, and then $A(n) = nB$. See also [1].

Fig. 2(a) shows the result of the calculation of $RS^{(1)}$ for the binary image shown in Fig. 1. It contains the point p and the segment $[c, q]$, where c is the same 'intralevel' redundant point shown in Fig. 1(c). The points from the segment (p, c), which are 'future-level' redundant in the skeleton, are not present in $RS^{(1)}$.

If we include in 'redundant region' of Eq. (12) the union of all the representation elements with order *smaller* than n as well, we obtain an error-free reduced skeleton, which we denote as $RS^{(2)}$, with *no interlevel redundancy*. The union of the representation elements with order smaller than n, which we denote as P_n, satisfies the following relation:

$$P_{n+\Delta n} = P_n \cup [RS_n^{(2)} \oplus A(n)], \quad n \geqslant 0,$$
$$P_0 = \emptyset. \tag{17}$$

Therefore, it can be computed recursively in the discrete case ($\Delta n = 1$). The subsets of $RS^{(2)}$ are given by

$$RS_n^{(2)} \triangleq X \ominus A(n) - (P_n \cup F_n) \ominus A(n). \tag{18}$$

Fig. 2(b) shows the result of the calculation of $RS^{(2)}$ for the same binary image as before. It contains only the points p, q and c. The points from the segment (c, q), which are interlevel redundant in the skeleton, are not present in $RS^{(2)}$. The point c, which is intralevel redundant, is still present.

To obtain a minimal skeleton, the intralevel redundancy should also be removed. Unfortunately, we still do not know how to define a 'redundant' region that would remove this kind of redundancy without affecting the property of exact reconstruction of the reduced skeletons. In the example of Fig. 2, the minimal skeleton (which is unique in this example) is shown in Fig. 2(c).

Fig. 3 shows the result of calculating the reduced skeletons defined above, for a real binary picture, the 256 × 256 'coffee grains'. Its skeleton, Fig. 3(a), was calculated using the shapes shown in Fig. 4 as the first six elements of $\{B(n)\}$, so that $\{A(n)\}$ is *approximately* a family of increasing *disks*, and the skeleton is as thin as possible. The other elements of $\{B(n)\}$ were derived from them cyclically by the formula: $B(n) = B(n \bmod 6)$. This skeleton contains 1360 representation points. Fig. 3(b) shows the reduced skeleton $RS^{(1)}$, containing 1145 points

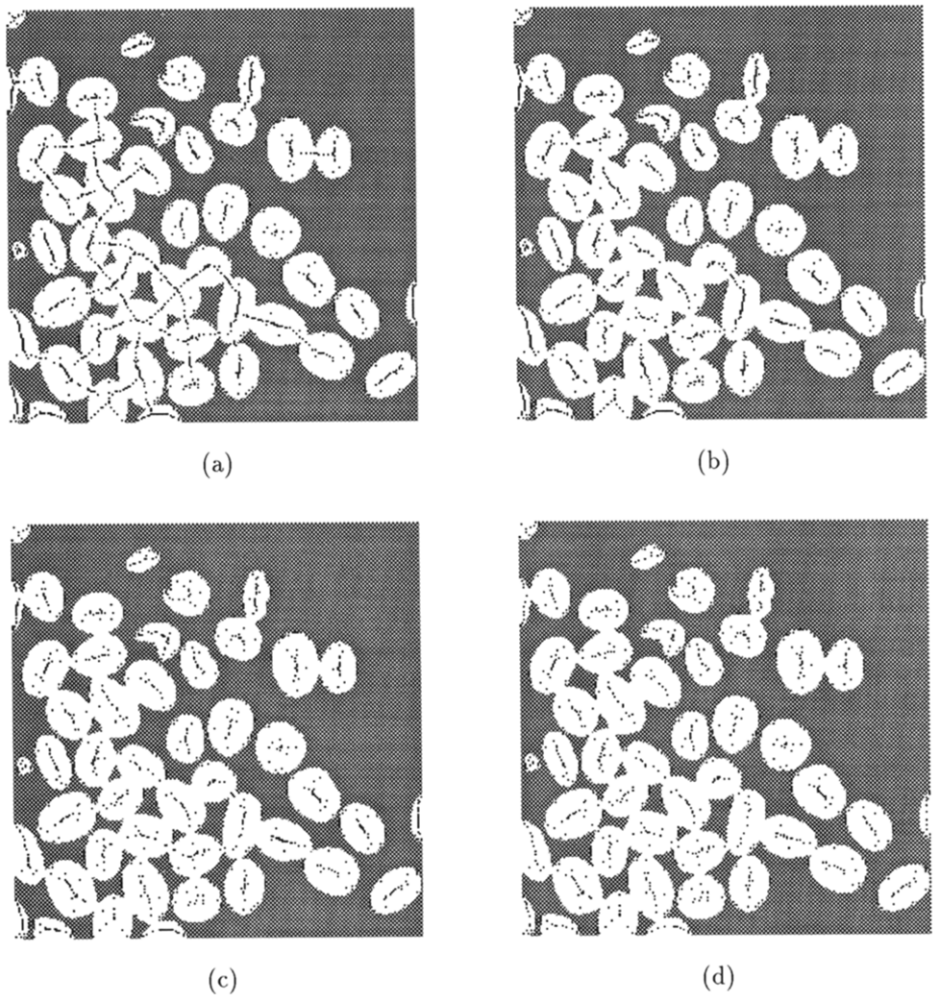

Fig. 3. Reduced skeletons. (a) Binary image and its skeleton, (b) its reduced skeleton $RS^{(1)}$, (c) its reduced skeleton $RS^{(2)}$, and (d) a minimal skeleton.

(15.8% less than the original skeleton), and Fig. 3(c) shows the reduced skeleton $RS^{(2)}$, containing 972 points (28.5% less than the original skeleton). For comparison, Fig. 3(d) shows a minimal skeleton, obtained with the non-morphological algorithm presented in [4]. It contains 877 points (35.5% less than the original skeleton). According to the above numbers, the reduced skeleton $RS^{(2)}$ was able to remove in this example 80% of the redundant points, using morphological operations only.

3. Extension to multi-structuring-element skeletons

In [2], we define and discuss some of the applications of the Multi-Structuring-Element Skeleton (MSES). The MSES is a generalization of the ordinary skeleton, using several families of shapes, instead of just one, to represent an image. It usually contains, after redundancy removal, considerably fewer representation points than an ordinary minimal skeleton, and these points are distributed in a richer parameter space [2].

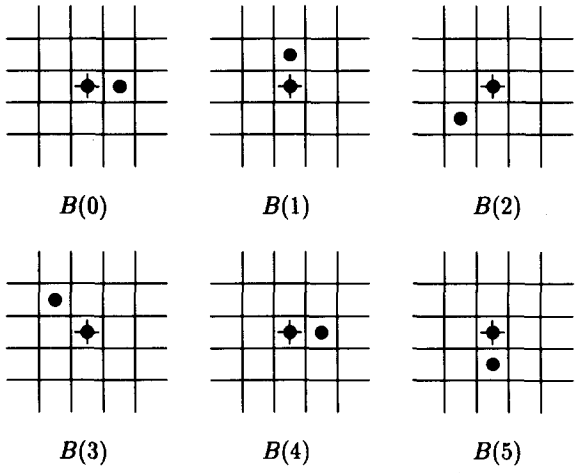

Fig. 4. Series of shapes $\{B(n)\}$ used in the calculations of the skeletons in Fig. 3 (The symbol + represents the origin).

In this section we present a generalized definition of the MSES, analog to the generalized skeleton above, and extend the approach developed in the last section, to obtain reduced MSES representations.

3.1. Definition of MSES

Like the ordinary skeleton, the MSES is composed of the center of the *maximal elements* picked from a given family of elements. The difference lies in the dimensionality of this family; for the ordinary skeleton, it is a 1-parameter family, whereas for the MSES, it is a multi-parameter family.

Given L series of shapes, $\{B_1(n)\}, \ldots, \{B_L(n)\}$, we generate the L-parameter family of shapes $\{A(\boldsymbol{n})\}$, where $\boldsymbol{n} = (n_1, \ldots, n_L)$ is an L-dimensional vector with non-negative components, in the following way:

$$A(\boldsymbol{n}) = A_1(n_1) \oplus A_2(n_2) \oplus \cdots \oplus A_L(n_L), \tag{19}$$

where each family $\{A_i(n)\}$, $1 \leqslant i \leqslant L$, is generated from $\{B_i(n)\}$, as in the generalized skeleton definition (10), by

$$A_i(0) = \{(0,0)\},$$

$$A_i(n + \Delta n) = A_i(n) \oplus B_i(n), \quad n \geqslant 0. \tag{20}$$

Fig. 5 shows two examples for the family $\{A(\boldsymbol{n})\}$. In both of them, $L = 2$ and the generating families are constant, i.e., $B_1(n) = B_1$ and $B_2(n) = B_2$, $\forall n$. In this case, $A(\boldsymbol{n}) = A(n_1, n_2) = n_1 B_1 \oplus n_2 B_2$.

The MSES's subsets S_n are then defined by

$$S_n = X \ominus A(\boldsymbol{n}) - \bigcup_{i=1}^{L} [X \ominus A(\boldsymbol{n})] \circ B_i(n), \tag{21}$$

where X is the original image. The subsets S_n contain the centers of maximal elements of 'size' $\boldsymbol{n}$.

The original image can be perfectly reconstructed from the collection $\{S_n\}$ according to the following formula:

$$X = \bigcup_{\boldsymbol{n}} S_n \oplus A(\boldsymbol{n}). \tag{22}$$

3.2. Reduced MSES

Reduced MSESs may be obtained from the same generic relation (11). For the multidimensional case, (12) should be written as

$$RS_n = \begin{pmatrix}\text{representation}\\ \text{region of order } \boldsymbol{n}\end{pmatrix} \ominus A(\boldsymbol{n}) - \begin{pmatrix}\text{redundant re-}\\ \text{gion of order}\\ \boldsymbol{n}\end{pmatrix} \ominus A(\boldsymbol{n}). \tag{23}$$

From this point on, until the end of the paper, we will restrict ourselves to the simplest case $L = 2$, and discrete parameters only, i.e., $\boldsymbol{n} = (n, m) \in \mathbb{N}^2$, where $\mathbb{N}$ is the set of natural numbers.

Similar to Section 2.3, we set 'representation region of order $\boldsymbol{n} = (n, m)$' to be $X \circ A(n, m)$. In order to produce a reduced MSES with no *future-level* redundancy (analog to (16)), and a reduced MSES with only *intralevel* redundancy (analog to (18)), we define $P_{n,m}$ and $F_{n,m}$, analogous to P_n and F_n defined in Section 2, as the union of the representation elements *smaller* than $A(n, m)$, and the union of the maximal elements *bigger* than $A(n, m)$, respectively. The concepts of *smaller* and *bigger* require the definition of a relation of order in $\mathbb{N}^2$, so we chose to use the *lexicographic* relation of order ($<$):

$$(a, b) < (c, d), \quad a, b, c, d \in \mathbb{N}, \tag{24}$$

$$(a < c) \text{ or } (a = c \text{ and } b < d).$$

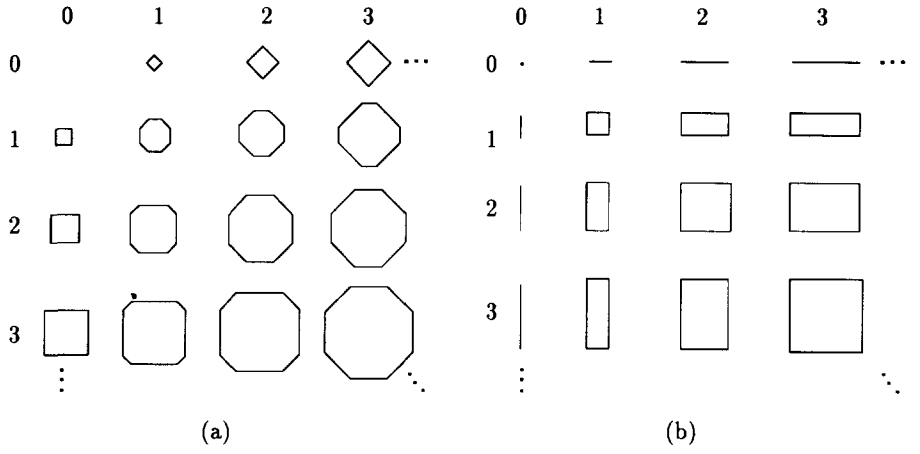

Fig. 5. Two examples for the family of shapes $\{A(n)\}$, for $L = 2$ and constant generators. (a) B_1 is a square and B_2 is rhombus, (b) B_1 is a unitary vertical line and B_2 is a unitary horizontal line.

The process of calculating the reduced MSES is done obeying the lexicographic order, in such a way that a subset $RS_{n,m}$ is not computed until all the subsets with index *smaller* than (n, m) are computed. After the set $RS_{n,m}$, the next subset to be computed will be $RS_{n,m+1}$, if $X \ominus A(n, m+1) \neq \emptyset$, or $RS_{n+1,0}$ otherwise.

$P_{n,m}$ are found recursively in the same way as P_n, 'accumulating' the representation regions $S_{n,m} \oplus A(n, m)$ for each step (n, m).

It can be shown that $F_{n,m}$ as defined above, can be computed at each step (n, m) by the formula

$$F_{n,m} = [X \circ A(n, m+1)] \cup [X \circ A(n+1, 0)]. \quad (25)$$

The reduced MSES, with no *future-level* redundancy, is hence defined as

$$RS^{(1)}_{n,m} \triangleq X \ominus A(n, m) - F_{n,m} \ominus A(n, m), \quad (26)$$

whereas the reduced MSES, with no *interlevel* redundancy, is obtained by

$$RS^{(2)}_{n,m} \triangleq X \ominus A(n, m) - (P_{n,m} \cup F_{n,m}) \ominus A(n, m). \quad (27)$$

3.3. Minimal MSES

For a particular but important choice of the families of shapes for the MSES with two structuring elements, formula (27) yields a representation with *no redundant points*, i.e., a minimal MSES. The families of shapes which provide this result are $A(n, m) = nB_1 \oplus mB_2$, where B_1 and B_2 are elements containing exactly two points, which we call *discrete elementary directional structuring elements*. The shapes in Fig. 4 are examples of discrete elementary directional structuring elements.

It is well known [4] that the ordinary skeleton, computed with any directional structuring element, contains no redundancy. As an extension to this property, the reduced MSES obtained in (27), computed with any pair of structuring elements from Fig. 4 (or any other pair of elementary directional elements), contains no *intralevel* redundancy.

Since the reduced MSES from (27) has no *interlevel* redundancy, the conclusion is that it contains no redundant points at all. It is therefore a minimal MSES.

In contrast to 1-parameter families of directional shapes, in which there is little interest as kernels, the families of shapes generated by pairs of elementary directional structuring elements are important ones. For example, in the case of the *horizontal* and the *vertical* elementary structuring elements (the first two elements shown in Fig. 4), the family $A(n, m)$ obtained is composed of all discrete rectangles (see Fig. 5(b)).

We compared the minimal MSES representation (given by Eq. (27)) of the binary image 'coffee grains' (Fig. 3) calculated with the horizontal and

vertical elementary structuring elements mentioned above, with a minimal skeleton representation of the same image calculated with a unit square as structuring element. Note that the 2-parameter family of rectangles, used for the MSES calculation, *contains* the 1-parameter family of squares, used for the skeleton calculation. In this case, the number of points in the minimal MSES is expected to be much smaller than the number of points in the minimal skeleton. Indeed, in the above simulation the minimal MSES obtained contains 708 points, whereas the minimal skeleton contains 990 points (a difference of 28.5%). The minimal skeleton calculation was performed using the non-morphological algorithm presented in [4].

4. Conclusion

A *morphological* approach for obtaining redundancy-reduced skeletons was presented. This approach is able to remove all the *interlevel* redundancy from the skeleton, leaving only *intralevel* redundant points. For MSES, and a particular but an important choice of the structuring elements, the approach provides a redundancy-free representation. A fully morphological method to compute a redundancy-free skeleton (minimal skeleton) in the general case, both for MSESs and for the ordinary skeleton, is still being sought.

Acknowledgments

We thank Dr. Serge Beucher for kindly providing us with the image 'coffee grains'. This work was supported by the Fund for the Promotion of Research at the Technion.

References

[1] J. Goutsias and D. Schonfeld, "Morphological representation of discrete and binary images", *IEEE Trans. Signal Process.*, Vol. 39, No. 6, June 1991, pp. 1369–1379.

[2] R. Kresch and D. Malah, "Morphological multi-structuring-element skeleton and its applications", *Proc. Internat. Symp. on Signal, Systems and Electronics*, Paris, September 1992, pp. 166–169.

[3] P. Maragos, "Pattern spectrum and multiscale shape representation", *IEEE Trans. Pattern Anal. Mach. Intell.*, Vol. 11, No. 7, July 1989, pp. 701–716.

[4] P. Maragos and R.W. Schafer, "Morphological skeleton representation and coding of binary images", *IEEE Trans. Acoust. Speech Signal Process.*, Vol. 34, No. 5, October 1986, pp. 1228–1244.

[5] I. Pitas and A.N. Venetsenapoulos, "Morphological shape decomposition", *IEEE Trans. Pattern Anal. Mach. Intell.*, Vol. 12, No. 1, January 1990, pp. 38–45.

[6] I. Pitas and A.N. Venetsenapoulos, "Morphological shape representation", *Pattern Recognition*, Vol. 25, June 1992, pp. 555–565.

[7] J.M. Reinhardt and W.E. Higgins, "Towards efficient morphological shape representation", *IEEE Internat. Conf. Acoust. Speech Signal Process. '93*, Vol. 5, April 1993, pp. V125–V128.

[8] G. Sapiro and D. Malah, "A geometric sampling theorem and its applications in morphological image coding", *Proc. Internat. Conf. Digital Signal Process.*, Florence, September 1991, pp. 410–415.

[9] G. Sapiro and D. Malah, "Morphological image coding based on a geometric sampling theorem and a modified skeleton representation", *J. Visual Commun. Image Representation*, Vol. 5, No. 1, March 1994, pp. 29–40.

[10] J. Serra, ed., *Image Analysis and Mathematical Morphology, Vol. 2, Theoretical Advances*, Academic Press, New York, 1988.